frontiers | Frontiers in Materials

TYPE Original Research
PUBLISHED 01 May 2025
DOI 10.3389/fmats.2025.1573222

OPEN ACCESS

EDITED BY
Luca Valentini,
University of Perugia, Italy

REVIEWED BY
Christian Demitri,
University of Salento, Italy
Kun Liang,
Nanyang Technological University, Singapore

*CORRESPONDENCE
Peng Wu,
pwu@tio.org.cn

†These authors have contributed equally to this work and share first authorship

RECEIVED 08 February 2025
ACCEPTED 21 April 2025
PUBLISHED 01 May 2025

CITATION
Li Y, Tang X, Liu Y, Chen X, Wang L, Su Y, He W, Li J, Huang Q and Wu P (2025) Advanced wound healing with chitosan hydrogels incorporating metabolites from whale-derived *Lactiplantibacillus plantarum* HJ-S2.
Front. Mater. 12:1573222.
doi: 10.3389/fmats.2025.1573222

Advanced wound healing with chitosan hydrogels incorporating metabolites from whale-derived *Lactiplantibacillus plantarum* HJ-S2

Yizhen Li[1,2†], Xu Tang[1,2†], Yang Liu[1,2†], Xiaofeng Chen[1,2], Ling Wang[1,2], Yanjun Su[3], Wei He[4], Jingjing Li[4], Qinmiao Huang[5] and Peng Wu[1,2*]

[1]Third Institute of Oceanography, Ministry of Natural Resources, Xiamen, China, [2]Fujian Provincial Key Laboratory of Island Conservation and Development (Island Research Center, MNR), Xiamen, China, [3]Stomatological Hospital of Xiamen Medical College, Xiamen, China, [4]China Tobacco Fujian Industrial CO., LTD., Xiamen, China, [5]Fujian Huijing Biological Technology CO., LTD., Zhangzhou, China

Introduction: Two significant barriers to skin wound care are severe inflammatory cascade reactions and microbial infections. The metabolites of probiotics contain various components, such as lactic acid and bacteriocins, which can synergistically maintain skin microecological balance and promote wound healing and tissue regeneration through mechanisms.

Methods: This study utilized lactic acid bacteria isolated from the whale intestine. Inspired by the concept of the whale's skin self-repair ability and the influence of gut microbiota on the skin, this study ingeniously utilized the acidic properties of the lactic acid bacteria fermentation broth to dissolve chitosan (CS), forming a hydrogel while simultaneously incorporating the cell-free probiotic metabolites (CFPM) of *Lactiplantibacillus plantarum* HJ-S2 into a stable three-dimensional network structure. Various characterizations were tested, including water content, swelling ability, rheological properties and degradability.

Results: This resulted in the creation of a medical hydrogel capable of promoting skin wound healing, named PM@CS hydrogel. PM@CS hydrogel exhibited excellent swelling ability in different liquid environment. FT-IR analysis showed that the hydrogel is successfully crosslinked, and thermalgravimetric analysis showed that PM@CS hydrogel was stably degraded under high temperature. PM@CS hydrogel and CFPM of HJ-S2 strongly inhibited the growth of *E. coli* and *S. aureus*. The organic acid content of CFPM was analyzed by HPLC, revealing the lactic acid and acetic acid were produced in large quantities as two main organic acid metabolites that may contribute to the antibacterial efficacy. Beyond the outstanding antibacterial ability, application of PM@CS hydrogel led to rapid healing of burn wounds, and diabetic wounds.

Discussion: The results indicated that the whale-derived probiotics have significant potential for application in treating burns and scalds, particularly in the treatment of diabetic wounds.

KEYWORDS

hydrogel, *Lactiplantibacillus Plantarum*, probiotic metabolites, burns, diabetic

1 Introduction

The skin plays the role as the guardian against external environment, preventing harmful substance and organisms from our body. Thus, when the skin is severely damaged, it may even become hard to maintain fluid homeostasis and body temperature, leading to serious consequences that may threaten one's life (Church et al., 2006).The process of wound healing is complicated, which involves inflammatory response, proliferative process and maturation period (Kamolz and Hecker, 2023). The typical characteristics of inflammatory phase are vasodilation, fluid extravasation and edema. Since the leukocytes and macrophages that initiate the proliferative process are recruited by inflammatory mediators (mainly cytokines) during inflammatory phase, it is quite important for successful wound healing as delayed wound healing with prolonged inflammation is likely to lead to scar formation (Rowan et al., 2015). Except for tissue damage, secondary infection caused by microorganisms is also a severe problem (Wang et al., 2018). However, the harm of bacterial infection on wounds has long been underestimated. Actually, wound infection is the biggest cause of death in patients suffering wound injuries (D'Abbondanza and Shahrokhi, 2021).

Burn wounds and chronic wounds are two common wound types. First, burns are a very common health issue all over the world. According to the WHO, there are over 10 millions of people suffer from burn wounds every year (Markiewicz-Gospodarek et al., 2022). Burn wounds can be caused by fire, electrics, lasers, radiations and chemicals like strong acid and strong base. According to the percentage of affected total body surface area (%TBSA) and the depth of the wounds, burns are classified into different degrees, which determine different nutrition supply and treatment strategy (Evers et al., 2010). Internationally, burn wounds are classified in the degree I-III. Degree I involves epidermis only. Degree IIa (superficial) involves papillary dermis while degree IIb (deep) involves reticular dermis (Abazari et al., 2022). Degree III involves the full thickness of skin, and even into the subcutaneous fat or deeper. For those patients who suffer third-degree burn, skin graft is urgently needed (Ozhathil et al., 2021). Furthermore, diabetic foot ulcers represent a prevalent form of chronic wounds, impeding wound healing and elevating the risk of infection due to neuropathy and vasculopathy resulting from chronic hyperglycemia. The management and treatment of diabetic foot ulcers have consistently constituted a significant challenge in the domain of clinical skin injury repair (Forbes and Cooper, 2013).

Wound dressing is a good alternative for wound patients when it is hard to operate skin graft. It contains many types including films, hydrogels, foams, hydrocolloids and so on (Broussard and Powers, 2013). Hydrogels can load drugs and ingredients that function in healing process, which play the role in antibacterial and anti-inflammatory process, maintaining the homeostasis of burn wound environment. Some hydrogel loading with cytokines can even control the response pathways and promote self-healing (Liang et al., 2021). Natural polymers, represented by chitosan, are optimal biomaterials for the fabrication of medical hydrogels, which exhibit superior characteristics in a range of biomedical applications. Chitosan is the sole natural alkaline polysaccharide that is found in significant quantities in nature. It is widely distributed in the exoskeletons of crustaceans and insects, and it can be obtained by deacetylation of chitin. The hydroxyl and amino groups present on the molecular chain of chitosan facilitate the formation of hydrogels through cross-linking, which exhibit favorable biophilicity and have the potential to act as hemostatics, antibacterial agents, and wound healing promoters (Khayrova et al., 2021; Younes and Rinaudo, 2015). Currently, chitosan-based medical wound dressings predominantly incorporate antibiotics or antimicrobial compounds, such as Ag^{+}, into their formulations (Peers et al., 2020; Chu et al., 2023). However, issues such as cytotoxicity impede their advancement due to the emergence of bacterial resistance. Consequently, alternative therapeutic approaches that do not rely on conventional antimicrobials are becoming increasingly crucial in wound management.

Probiotics are defined as live microorganisms that exert beneficial effects on the host when administered in adequate amount. It has long been reported that probiotics and their metabolites play a role in the regulation of human health by affecting the microbiota (Liu et al., 2023; Marco et al., 2017; Wieërs et al., 2019). As the microbiota of wound area have a conclusive effect on the wound environment and wound healing process, probiotics and their metabolites have the potential to be applied to the regulation of the wound microbial environment (Uberoi et al., 2024). For example, *Lactiplantibacillus plantarum* has the capacity to impede the proliferation of pathogenic microorganisms, including *Staphylococcus aureus* and *Pseudomonas aeruginosa*, through the production of extracellular products (probiotic metabolites, PM) that contain antimicrobial substances, such as organic acids, polysaccharides and bacteriocins (Li et al., 2023; Al-Saafin et al., 2023). The antimicrobial substances in PMs were reported to disrupt the cell morphology and interfere multiple metabolic pathways of the pathogens (Rao et al., 2024). This may serve as a therapeutic aid to antibiotics and Ag^{+} based products as alternative treatments. Besides, as it is reported, the gut-skin axis is highly related to wound healing process, as the gut impact the skin due to its immunological and metabolic properties (Patel et al., 2022). From a bionic point of view, the environment in which whales live is prone to skin injuries. As a result, they have developed a robust ability to heal themselves from wounds (Womersley et al., 2021). Microorganisms present in the whale gut may contribute to the repair of skin tissue through the gut-skin axis. In 2017, our research

team successfully isolated a strain of *Lactobacillus plantarum* named HJ-S2 from the gut samples of a *Mesoplodon densirostris* that had stranded on Ningde Beach in Fujian, China. After a preliminary study, it has been reported that *L.plantarum* HJ-S2 possessed cholesterol-lowering function (Wan et al., 2023). The ability to lower cholesterol may promote wound healing process by improving macrophage motility (Zhao et al., 2023a).

The ocean represents one of the most biodiverse ecosystems on Earth. However, owing to the unique characteristics of its environment and the challenges associated with resource exploitation, a significant portion of its biological resources remains undeveloped. In recent years, marine probiotics have begun to be explored and have gradually entered the public domain (Kim et al., 2012). Marine probiotics are involved in the production of inhibitory substances which prevent the adhesion of pathogens to the intestinal epithelium, direct inhibition of Gram-negative bacteria, regulation of short-chain fatty acids, downregulation of proinflammatory cytokines, colonization of intestinal permeability, regulation of electrolyte adsorption, maintenance of the immune response of the intestine, and maintenance of lipid metabolism (Eze et al., 2023). Despite the numerous advantages of marine probiotics, their difficult sample collection and strain screening pathways are the most critical factors limiting development. At the same time, due to the special temperature and pressure environment of the ocean environment, many marine probiotics tend to be halophilic, psychrophilic or barotropic, thus the culture conditions are relatively harsh. This resulted in a large number of potential probiotic strains that could not be isolated for culture (Peixoto et al., 2021).

Other researchers have incorporated probiotics into hydrogels to achieve functions such as regulating gut microbiota and enhancing wound healing (Mei et al., 2022; Kuhn et al., 2024; Liu et al., 2023, Ming et al., 2021). However, there is a notable lack of studies focusing on the incorporation of marine-derived probiotics into hydrogels.In this study, cell-free probiotic metabolites (CFPM) of *L.plantarum* HJ-S2, derived from the intestinal samples of *M. densirostris*, were loaded onto a chitosan-based hydrogel (PM@CS), and evaluated for their antimicrobial capacity and effects on burn wound healing and chronic wound healing caused by hyperglycemia (Figure 1), with the objective of identifying novel solutions for the inhibition of wound infections and promotion of healing.

2 Materials and methods

2.1 Materials

Lactiplantibacillus plantarum HJ-S2 was isolated from the intestinal contents of *M. densirostris* stranded in China (Ningde, Fujian Province) in October 2017. For convenience, the term "HJ-S2" will be used to refer to *Lactiplantibacillus plantarum* HJ-S2 throughout this paper.

De Man, Rogosa and Sharpe (MRS) culture medium used to culture HJ-S2 were prepared as follows: peptone (10.0 g), glucose (20.0 g), beef extract (10.0 g), yeast extract (5.0 g), sodium acetate (5.0 g), sodium dihydrogen phosphate (2.0 g), diammonium hydrogen citrate (0.5 g), magnesium sulfate (0.58 g), manganous sulfate (0.25 g) and Tween-80 (1.0 mL). These ingredients were dissolved in 1 L H_2O, and the pH was adjusted to 6.2 to 6.4. After that, the medium was sterilized at 121°C for 20 min. Then the medium was cooled to room temperature and stored for future use.

Luria-Bertani (LB) culture medium used to culture *E.coli* and *S.aureus* contains tryptone (10.0 g), sodium chloride (10.0 g), yeast extract (5.0 g). The ingredients were dissolved in 1 L H_2O, and the pH was adjusted to 7.2 to 7.4. The medium was sterilized at 121°C for 20 min. Then the medium was cooled to room temperature and stored for future use.

The Sprague-Dawley (SD) rats and db/db mice used for animal experiments were purchased from Slac Laboratory Animal Co., Ltd. (Shanghai, China).

2.2 Hydrogel preparation through the combination of cell-free probiotic metabolites and chitosan

First, HJ-S2 was cultured to collect its cell-free probiotic metabolites (CFPM): 2 mL of overnight HJ-S2 culture in the test cube (aged 24 h) was inoculated into 100 mL of MRS broth and kept for 48 h at 37°C in a shaking incubator. After incubation, the culture was centrifugated at 9,500 rpm for 30 min. The resulting liquid supernatant was collected, and any remaining bacteria were removed using a 0.22 μm Millipore filter (Mekky et al., 2022).

Second, a 2% (ω/w) PM@CS solution was prepared by dissolving 2 g of chitosan (deacetylation degree = 95%, purchased from Qingdao Biotemed Biomaterials Co., Ltd.) in 100 mL cell-free PM. Otherwise, a 2% Pure CS solution was prepared by dissolving 2 g of chitosan in 100 mL 0.1 M acetic acid instead. The solutions were stirred overnight and then centrifuged at 3,000 rpm for 10 min to remove insoluble substances.

Third, genipin as the crosslinking agent was dissolved in ethanol to form a solution of 5 mg/mL (Heimbuck et al., 2019). Then, the PM@CS solution and genipin solution were mixed at a ratio of 2.5%, 2%, 1.5% and 1% (w/v of genipin to chitosan, respectively). Separately, Pure CS solution was mixed with genipin solution to form the precursor of Pure CS hydrogel. The mixtures were centrifugated at 2,000 rpm for 5 min. The resulting supernatant was poured into different molds and incubated at 37°C for 24 h to form hydrogel. The hydrogel samples with different chitosan and genipin ratios are labeled as shown in Table 1.

2.3 Scanning electron microscopy (SEM) analysis

The internal structure of the hydrogel was observed using SEM. Various hydrogel samples were immersed in deionized water for 24 h to preserve their original pore structure. Subsequently, surface moisture was removed using filter paper. Then the samples were broke brittlely by liquid nitrogen to show perfect cross-section structure. The porous characteristics were analyzed by a Quanta 450 Field Emission Scanning Electron Microscope (FEI, USA).

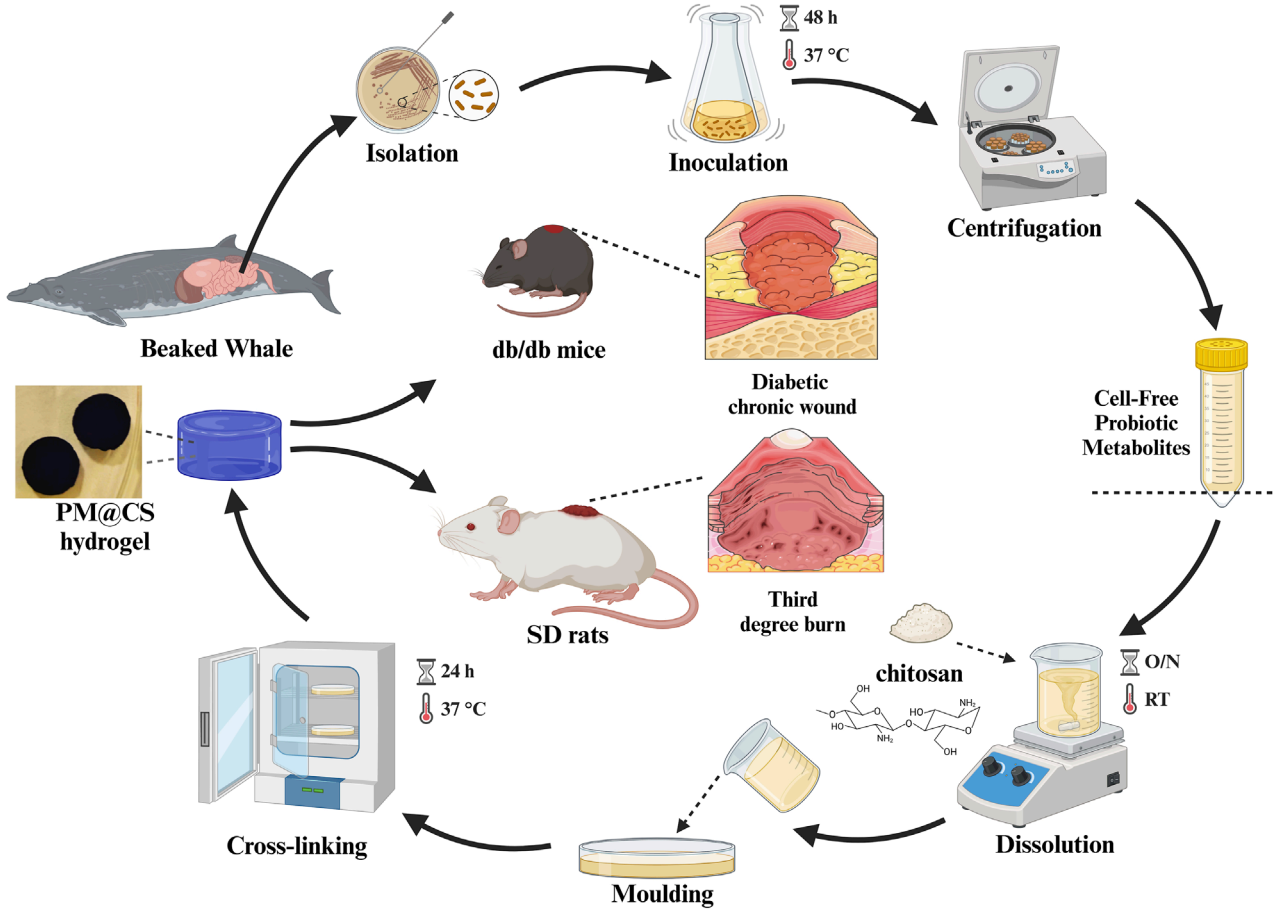

FIGURE 1
Synthesis of PM@CS hydrogel and the animal test of PM@CS hydrogel on various type of wounds: burn wound and diabetic chronic wound. Created in BioRender. Li, Y. (2024) https://BioRender.com/p39e022.

TABLE 1 Formulations of PM@CS hydrogel.

Sample	PM@CS solution (mL)	Pure CS solution (mL)	Genipin solution (mL)	H_2O (mL)	w/w of genipin to chitosan
PM@CS	10	—	1	—	2.5%
PM@CS-b	10	—	0.8	0.2	2%
PM@CS-c	10	—	0.6	0.4	1.5%
PM@CS-d	10	—	0.4	0.6	1%
Pure CS	—	10	1	—	2.5%

2.4 Thermalgravimetric (TGA) analysis

The thermal stability of different formulations of PM@CS hydrogel and Pure CS hydrogel was evaluated using a TGA3 analyzer (Mettler Toledo, USA) under a nitrogen atmosphere. Initially, the hydrogels were lyophilized and ground into a fine powder. Subsequently, 1.5 mg of each hydrogel powder sample was placed in the analyzer. The testing protocol involved a heating rate at 10°C/min up to 550°C with the residual mass recorded in real-time. Both the weight loss curve (TG curve) and its first derivative (DTG curve) were calculated.

2.5 Rheological test

Rheological measurements were employed to characterize the mechanical properties and strength of the biologically crosslinked hydrogels. The rheological properties of the hydrogels were evaluated using a Discovery DHR-2 rheometer (Waters TA Instruments, USA). The tests were conducted in accordance with previously established methods (Li et al., 2024; Priddy-Arrington et al., 2023). The precursor of each hydrogel was cast into a 90 mm disc mold and subjected to crosslink process at a temperature of 37°C for 24 h. Subsequently, the hydrogel was immersed in deionized water for 24 h to maintain its water content. Firstly, the linear viscoelastic region (LVR) of hydrogels was determined. Dynamic amplitude sweeps were performed with a specified strain range of 0.001–0.1 at an angular frequency of 10 rad/s. The storage modulus (G′) and loss modulus (G″) were then determined by varying the frequency between 1 and 100 rad/s at a certain temperature of 25°C. The effects of temperature on the storage modulus and loss modulus were assessed at a deformation within the LVR of the hydrogel and a constant angular frequency of 10 rad/s. The temperature was incrementally increased from 15°C to 65°C to evaluate the stability of hydrogels under different thermal conditions. A Peltier temperature control unit was utilized to measure and regulate the temperature of the rheometer plate. To ensure accurate measurements, the thickness of the hydrogel samples was maintained at 700 ± 50 μm. Three hydrogel sample from each group was tested to determine the average moduli.

2.6 Fourier transform infrared (FT-IR) analysis

The PM@CS hydrogel and Pure CS hydrogel was lyophilized and grinded into a fine powder. The sample powder and KBr powder were mixed at the ratio of 1:100 under infrared light. The structural and functional groups analyses of the PM@CS hydrogel, Pure CS hydrogel and uncrosslinked CS were subsequently conducted using a FT-IR Spectrometer in the range of 4,000–400 cm^{-1}, with a scan count of 32, a resolution of 8 cm^{-1}.

2.7 Swelling ratio

To evaluate the water absorption and swelling behavior of PM@CS hydrogel, the rate of water loss and swelling ratio was assessed as follows. Firstly, the hydrogel was weighed (m_0) and lyophilized to remove water content, with the post-lyophilization weight recorded as m_1. Then the lyophilized hydrogel was immersed in deionized water, simulated body fluid (SBF, purchased from Shanghai yuanye Bio-Technology Co., Ltd.), high glucose DMEM culture medium (purchased from Beijing Solarbio Technology Co., Ltd.) for 24 h to achieve swelling equilibrium. At specific intervals, surface water was blotted from the hydrogels, and they were reweighted as m_2. The water content and swelling ratio of PM@CS hydrogel were then calculated as follows:

$$\text{Water content}\,(\%) = \frac{m_2 - m_1}{m_1} \times 100$$

$$\text{Swelling ratio}\,(\%) = \frac{m_2 - m_1}{m_1} \times 100$$

2.8 *In vitro* degradation test

To evaluate the self-degrade and enzymatic degradation capabilities of PM@CS hydrogel, PM@CS hydrogel and Pure CS hydrogel were fabricated into circular slices (Φ = 12 mm). The initial weight (m_0) of each sample was recorded prior to immersion in various solutions: deionized water, simulated body fluid (SBF, purchased from Shanghai yuanye Bio-Technology Co., Ltd.), and lysozyme (LYZ, 2 μg/mL, purchased from Shanghai Macklin Biochemical Technology Co., Ltd.). At predetermined time points (day 1, 3, 5 and 7), the residual portion of each sample was extracted from the solution. Surface moisture was carefully removed, and the samples were re-weighed (m_n). The immersion solutions were completely refreshed daily to maintain consistent degradation conditions. The *in vitro* degradation rate at day n was calculated using the following formula:

$$\text{Degradation grade}\ (\%) = \frac{m_n}{m_0} \times 100$$

2.9 Antibacterial test

The antibacterial activity was evaluated using the Agar Well Diffusion method. Prior to sterilization, agar was incorporated into LB broth at a concentration of 18 g/L. Following sterilization, the medium was allowed to cool to 55°C, at which point 1 mL of overnight culture of *Escherichia coli* and *S. aureus* was individually inoculated into 100 mL of the medium. The inoculated mixture was subsequently dispensed into sterile Petri dishes. Wells with a diameter of 10 mm aseptically created in the solidified agar plate. Aliquots (100 μL) of each test sample were carefully introduced at 37°C for 24 h. Following incubation, the diameter of the inhibition zone were precisely measured using a vernier caliper.

2.10 Organic acid characterization in cell-free probiotic metabolites (CFPM)

In order to analyze the composition of organic acids in CFPM, we quantitatively measured the contents of three common short-chain fatty acids (acetic acid, propionic acid, butyric acid) and lactic acid, the major fermentation products of lactic acid bacteria, by HPLC using a Waters Alliance Separations module e2695 coupled to a Waters 2,414 refractive index detector (Waters Corporation, USA). Samples or standards were injected into a Aminex HPX-87H Ion Exclusion Column (300 mm × 7.8 mm, Bio-rad Laboratories, Inc., USA) operated at 40°C The samples were eluted with H_2SO_4 (0.005 mM) at a flow rate of 0.6 mL/min. Sample detection was performed by comparing retention times of standards. Analytical grade acetic acid, propionic acid, butyric acid, and lactic acid (purchased from Shanghai ANPEL Laboratory Technologies Inc.,China) were used as standards. The assay was performed in triplicate.

2.11 *In vivo* healing performance on burn wound

The experimental method was adapted from Oryan's method (Oryan et al., 2019). All protocols were approved by the Institutional Committee on the Care and Use of Animals of the Third Institute of Oceanography, Ministry of Natural Resources.To investigate the effect of PM@CS hydrogel on the recovery of burn wounds, the model of third-degree burns was established on SD rats. First, the rats were divided into four groups, and the back of the rats were shaved with a shaver to remove the hair and expose the skin. Stainless steel cylinders with a diameter of 2.5 cm were heated in boiled water for 20 min. Then the cylinders were placed firmly against the rat's back for 15 s to form circular wounds, twice on each rat. Drug administration started 6 h after modeling. 500 μL of PM@CS, Pure CS hydrogel and cell-free PM (CFPM) of HJ-S2 were applied to the wound area, once per day for 28 days. Human epidemical growth factor (EGF) gel (purchased from Guilin Pavay Gene Pharmaceutical Co., LTD.) was used as positive control. The model group was given equal amount of saline. Photos of the wound area were taken at day 1, 4, 7, 10, 14, 21 and 28 to record the healing process of each group.

To further investigate the efficiency of wound closure, histopathology analysis of wound area was conducted by harvesting the skin tissue of wound area at day 28, for further H&E staining, Masson staining and immunohistochemical analysis.To qualitatively detect the expression of immune factors and proteins associated with tissue regeneration, IHC profiler, a open source plugin of ImageJ (National Institutes of Health, USA) was ultilized to assess the immunohistochemical staining images and give a quantitative relative IHC score related to the level of expression (Varghese et al., 2014).

2.12 *In vivo* wound healing performance on diabetic chronic wound

The experimental method was adapted from Grip's method (Grip et al., 2021). All protocols were approved by the Institutional Committee on the Care and Use of Animals of the Third Institute of Oceanography, Ministry of Natural Resources.The effect of PM@CS hydrogel on diabetic wound healing was studied using the genetic leptin-resistant db/db mice, which exhibited type II diabetes. Db/db mice were divided into five groups, the back of the mice was shaved and punched with biopsies puncture apparatus (Φ = 8 mm), four times each individual. Drug application started at the next day after wounded. 100 μL of PM@CS hydrogel, Pure CS hydrogel and cell-free PM of HJ-S2 were applied to the wounds, twice per day for 14 days. Human epidemical growth factor (EGF) gel was used as positive control. The model group was given equal amount of saline. To record the wound healing process, photos of the wound area were taken at day 1, 3, 5, 7, 10 and 14. The initial wound area (A_0) and the wound area within the 14 days administration process (A_n) was measured by ImageJ, and the wound healing rate was calculated as follows:

$$\text{Wound healing rate}\,(\%) = \frac{A_0\text{-}A_n}{A_0} \times 100$$

After 14 days' administration, skin tissues of wound area were taken for H&E staining and Masson staining to examine the wound healing histologically.

2.13 Statistical analysis

Data were analyzed with GraphPad Prism 8 (GraphPad Software, Inc., La Jolla, CA, USA). The data related to water content and rheological test are displayed in terms of the average ± standard deviation. The tests were repeated in triplet, with the average values recorded. Statistical comparisons between different groups were done using one-way analysis of variance (one-way ANOVA test), and the differences were considered significant at $P < 0.05$ (*), $P < 0.01$ (**), $P < 0.001$ (***) and $P < 0.0001$ (****).

3 Results and discussions

3.1 Characterization of PM@CS hydrogels

The internal pore structures of various hydrogel formulations were shown in Figures 2A–E. Alteration in the genipin in PM@CS hydrogel demonstrated a notable impact on the hydrogels' porous structure. PM@CS, PM@CS-b and Pure CS hydrogels exhibited more fully developed pore structures, whereas those with PM@CS-c and PM@CS-d displayed incomplete internal porous networks. Quantitative analysis of the porous structure was conducted using ImageJ software, with results presented in Figure 2F. The findings indicate that as the proportion of the cross-linking agent is reduced, the internal pore diameter of the hydrogel increases, resulting in a more pronounced loosening of the porous structure. These finding suggest that hydrogels prepared with CFPM of HJ-S2 exhibit a greater degree of porosity within their structure than Pure CS hydrogel, and display a greater diversity of characteristics. Crosslinking with a sufficient concentration of genipin facilitates the formation of a more comprehensive internal structure in hydrogels without significantly compromising their overall porosity.

The thermogravimetric (TG) and derivative thermogravimetric (DTG) curves of PM@CS hydrogels with varying formulations were shown in Figures 3A,B, respectively. The thermal degradation of PM@CS hydrogel can be characterized by three different stages. The initial weight loss observed below 110°C was attributed to the evaporation of free water. In the temperature range of 110°C–230°C, the weight loss is primarily due to the elimination of bound water and the onset of degradation in shorter chains. The third stage, occurring between 230°C and 390°C, was associated with the decomposition of chitosan polymers.The impact of varying genipin ratios on the hydrogel's thermal stability is illustrated using different colors in the thermograms. All hydrogel formulations, with the exception of PM@CS-d, exhibited thermal stability at elevated temperatures. When the temperature exceeded 390°C, the PM@CS-d formulation demonstrated rapid degradation, while the other formulations maintained their stability. It can be inferred that when the addition of genipin is lower than a certain proportion, the thermal stability of the gel will decrease significantly.By integrating SEM images with thermogravimetric analysis results, it can be concluded that the PM@CS-d hydrogel is not an

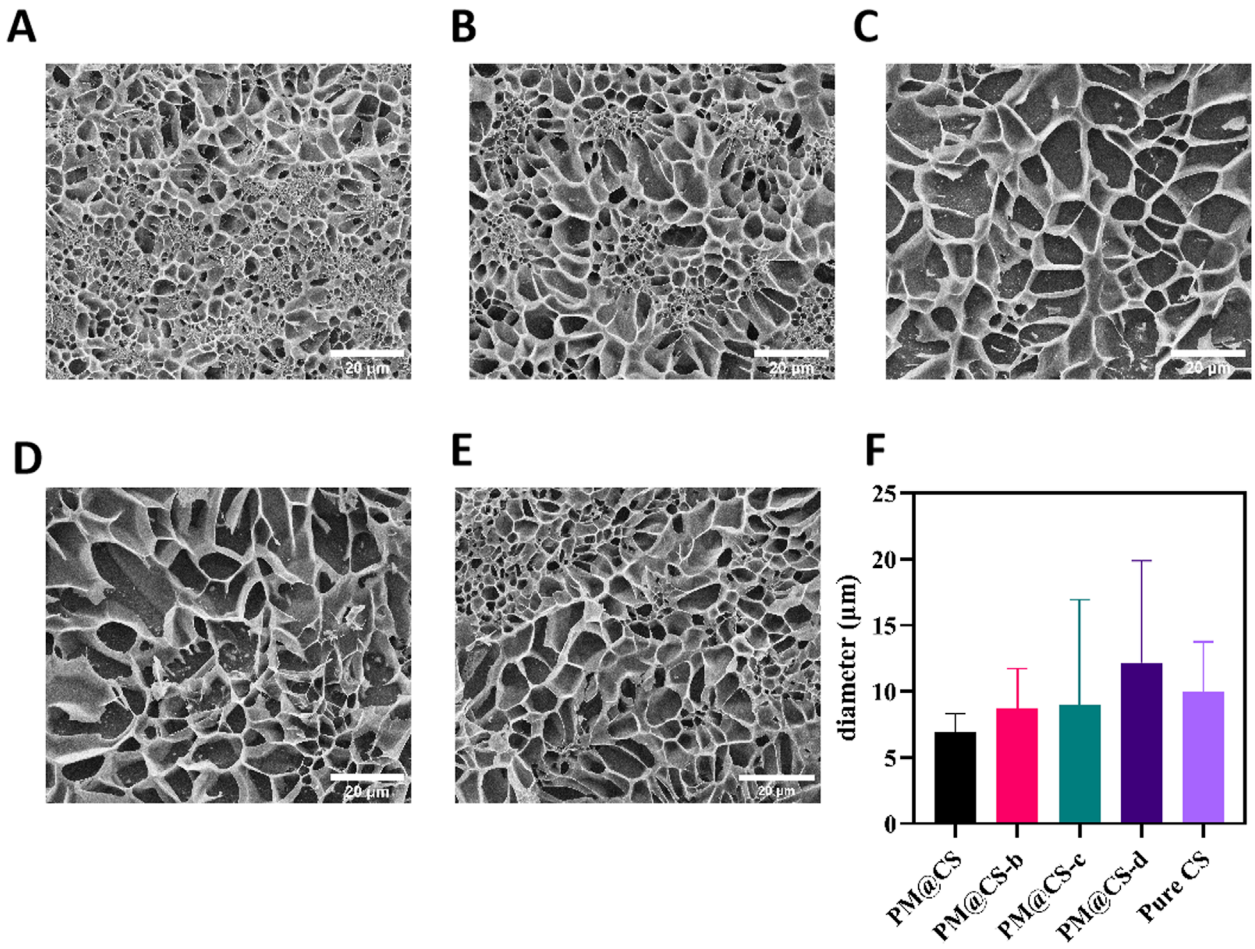

FIGURE 2
Morphological characteristics and water absorb ability of PM@CS hydrogel. **(A–D)** SEM images of **(A)** PM@CS, **(B)** PM@CS-b, **(C)** PM@CS-c, **(D)** PM@CS-d, and **(E)** Pure CS hydrogel. **(F)** Internal porous structure diameter of hydrogels.

appropriate formulation owing to its incomplete internal structure and insufficient thermal stability. This is primarily attributed to the low proportion of genipin crosslinker, which results in an unstable internal structure.

To further investigate the impact of varying genipin concentrations on gel properties, the dynamic rheological analysis on different groups of hydrogels was performed to provided quantitative information about the viscoelastic properties of each hydrogel. To find out the linear viscoelastic region (LVR) of PM@CS hydrogel, a sweep was conducted at the oscillation angular frequency of 10 rad/s (Figure 3C). The ratio of loss modulus (G″) to storage modulus (G′), which was called loss tangent, remained at a steadily numerical value at the strain between 0 ~ 4 %, while the loss tangent value increased moderately between 4 ~ 10%, and then rapidly after exceeding 10%. It was confirmed that the hydrogel was in its LVR when the strain was less than 4%. Following the identification of the LVR of PM@CS hydrogel, the strain was confirmed for the subsequent frequency and temperature scans. Based on the determined range of the LVR for the hydrogel, the strain was maintain at 1% for subsequent analyses.

Frequency-modulus curves revealed that within the angular frequency range of 0.1 ~ 100 rad/s, the storage modulus (G′) of all samples exhibited a pronounced plateau, significantly exceeding the corresponding loss modulus (G″) values (Figure 3D). Notably, fluctuations in vibrating frequency between 1 ~100 rad/s did not induce any discernible effect on the hydrogel's storage modulus. However, this trend was not mirrored in the loss modulus behavior. With the exception of the PM@CS hydrogel formulation, all other all other compositions demonstrated consistent behavior: their loss modulus remained relatively constant within 0.1 ~ 1 rad/s, followed by a steady increased in the 1 ~ 100 rad/s range. Thermal variations within the range of 15°C–65°C did not elicit any significant alterations in the hydrogels' modulus (Figure 3E). Frequency-modulus analyses indicated that the PM@CS hydrogel exhibited superior stability under vibrational stress compared to other formulations, suggesting enhanced resistance to external forces. Figure 3F illustrates the mean G′ and G″ values across the frequency spectrum for the hydrogel formulations. The PM@CS hydrogels demonstrated markedly elevated G′ and G″ values relative to the PM@CS-b and PM@CS-c hydrogel compositions. The similar G′

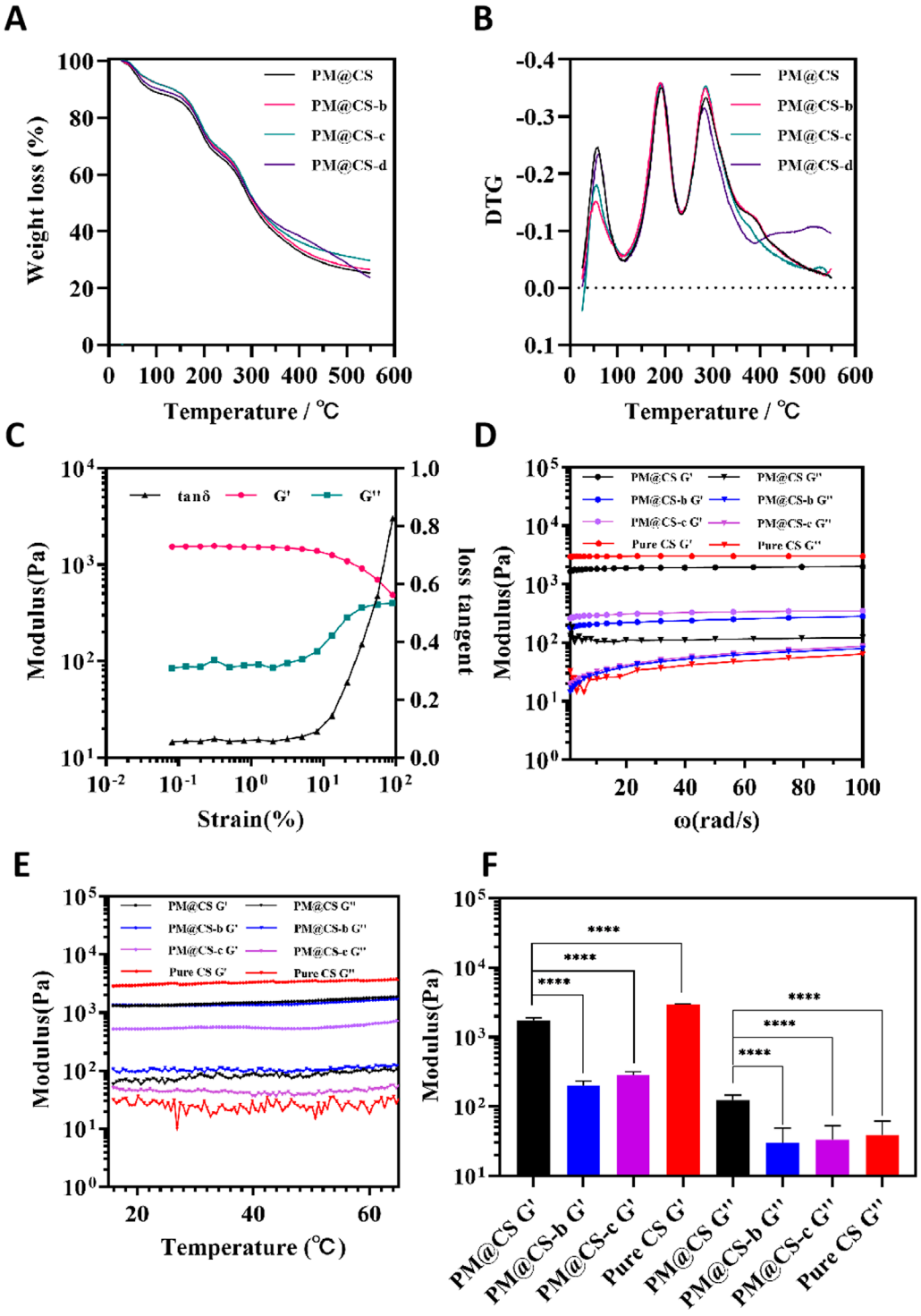

FIGURE 3
Characterization of different formulations of hydrogel. **(A)** TG curve and **(B)** DTG curve of hydrogels in different formulations. **(C)** Determination of LVR of PM@CS hydrogel. **(D)** Frequency sweep of hydrogels. **(E)** Temperature sweep of hydrogels. **(F)** Average modulus of hydrogels.

and G″ values and trends were reported by Priddy-Arrington et al. In their research, a injectable in-situ crosslinked chitosan hydrogel was developed and showed great potential in medical care (Priddy-Arrington et al., 2023). These findings substantiate the versatility of the PM@CS hydrogel system, indicating its potential for diverse application scenarios through precise modulation of its formulation. This allows for tailored adjustment of mechanical properties while maintaining structural integrity.

FT-IR spectra of PM@CS compared to Pure CS hydrogel was shown in Figure 4A. The broad peak around 3,300 cm^{-1} is assigned

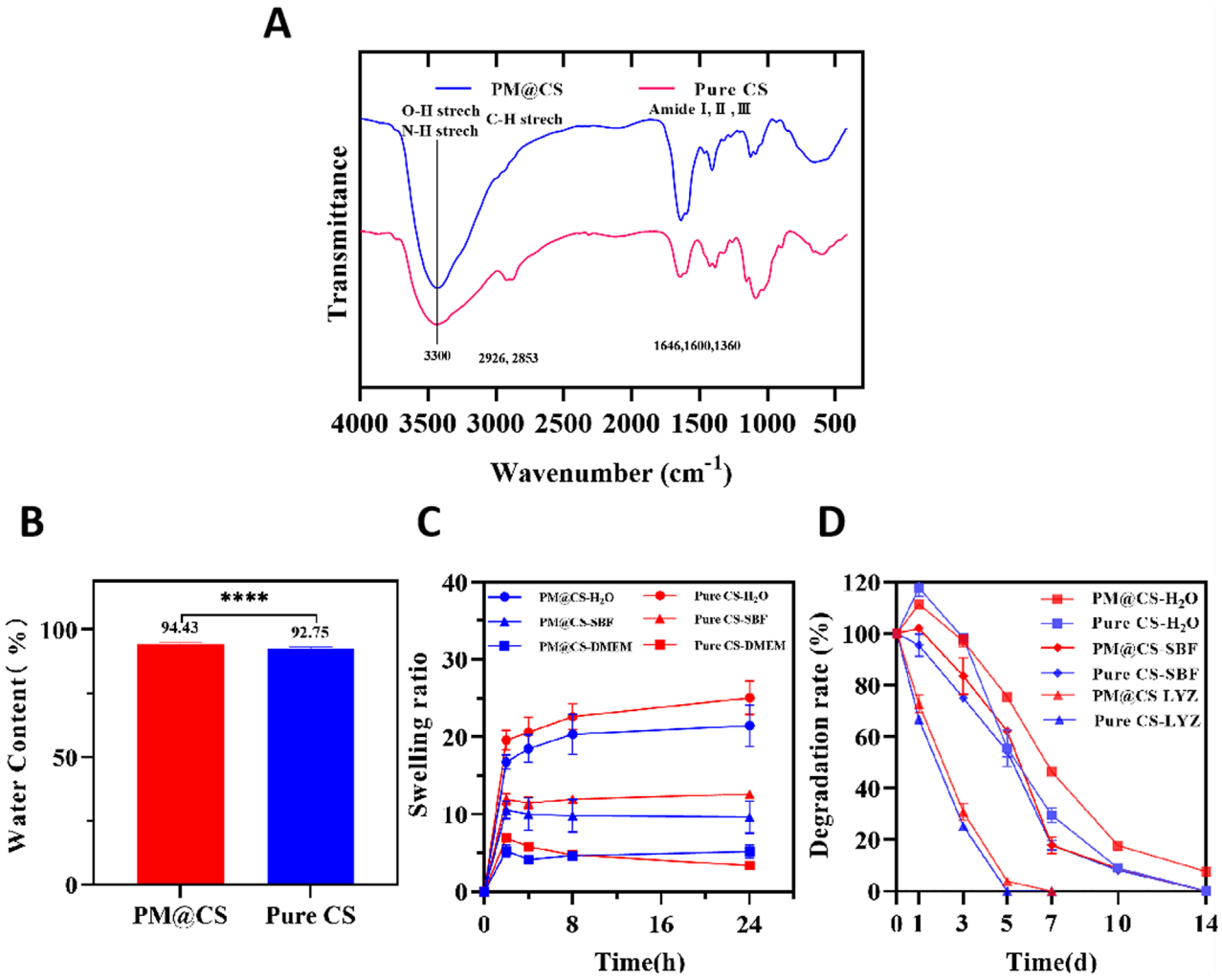

FIGURE 4
FT-IR analysis, swelling ability and biodegradability of PM@CS hydrogel. **(A)** FT-IR spectra of hydrogels and uncrosslinked CS. **(B)** Water content of PM@CS hydrogel and Pure CS hydrogel. **(C)** Swelling ability in different medium. **(D)** Degradation curve of hydrogels in water (H_2O), simulated body fluid (SBF) and lysozyme (LYZ).

to O–H stretching and N–H stretching. The peaks at 2,926 cm^{-1} and 2,852 cm^{-1} belong to asymmetric and symmetric stretching vibration of–CH_2 group, and peaks at 1,646,1,600 and 1,360 cm^{-1} to amide I, amide II and amide III as well as NH_2 bending, respectively. The intensity of peaks at 1,646 cm^{-1} (amide I) and 1,600 cm^{-1} (amide II) increased compared to Pure CS hydrogel. The difference is assigned to the enhanced formation of imine bonds by crosslinking between amino groups of CS and genipin (Andrade Del Olmo et al., 2022). The result suggested that both PM@CS and Pure CS hydrogel were well-crosslinked, and by connectively combination betweeen CS and genipin, PMs of HJ-S2 strengthened the internal crosslinking of the hydrogel. The attenuation of C-H vibrations may be attributed to the influence of complex proteins, organic acids, and peptides present in the CFPM of HJ-S2 on the assay.

Figures 4B,C illustrated the water content and swelling characteristics of the hydrogels, in different solution respectively. Here, simulated body fluid (SBF) is employed to mimic the composition of human plasma, while DMEM medium is utilized to replicate the microenvironment for wound cell regeneration. Additionally, water, which wounds may encounter in daily life, is also considered. These distinct solutions collectively simulate the diverse environments to which hydrogels could be exposed during their applications. Experimental results demonstrated that PM@CS hydrogel exhibited lower swelling capacity compared to pure chitosan hydrogel in both deionized water and simulated body fluid (SBF). While in DMEM medium, the swelling capacity of PM@CS hydrogel was significantly superior than Pure CS hydrogel. The dissolved solid matter in the HJ-S2 cell-free PM (CFPM) might have influenced the water absorption capacity of the hydrogel. On one hand, we observed that PM@CS hydrogel possessed superior fluid retention capability in cell culture environments compared to Pure CS hydrogel, indicating its adaptability to wound environments. It suggested that PM@CS hydrogel possesses enhanced compatibility with the cellular growth environment and has potential to absorb greater amounts of wound exudate (Gong et al., 2023). On the other hand, the low swelling properties of PM@CS hydrogel in other

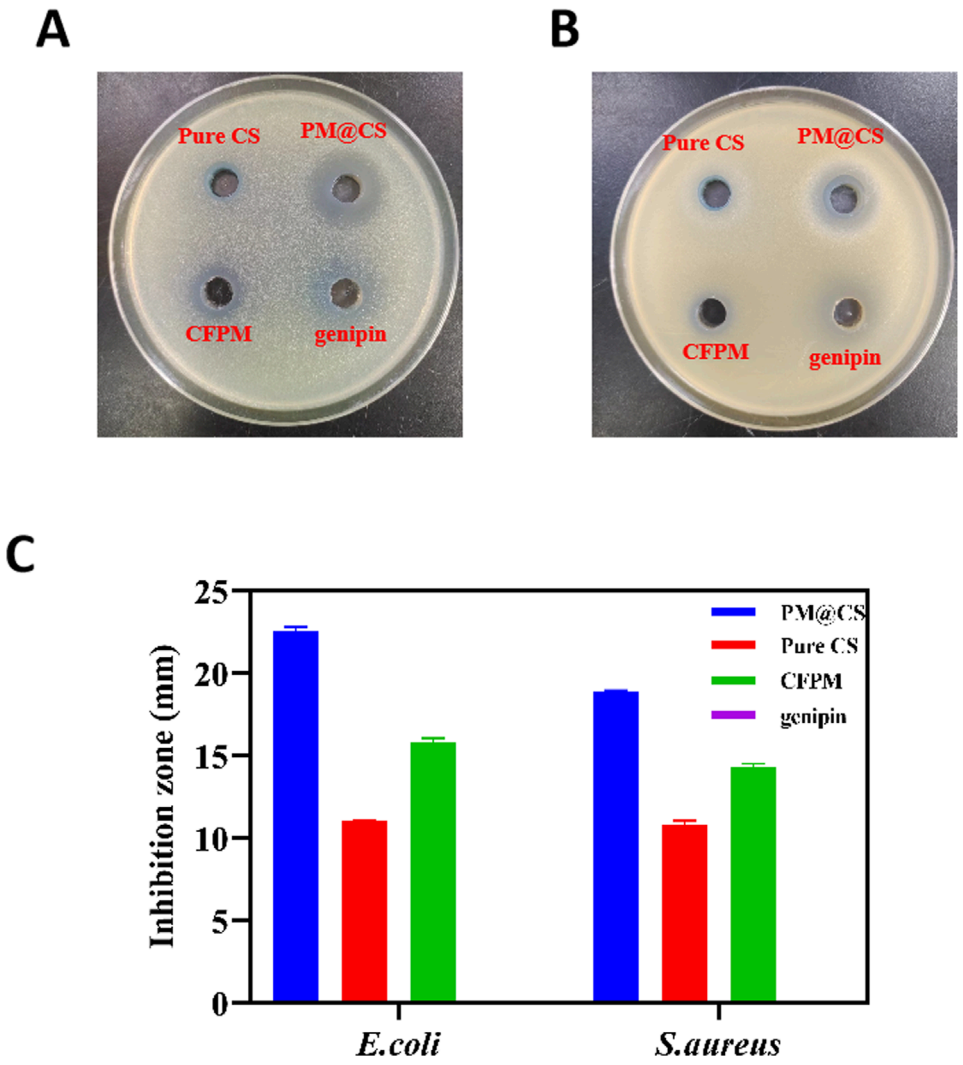

FIGURE 5
Antibacterial tests of the hydrogels. The antibacterial ability of PM@CS hydrogel (upper right), Pure CS hydrogel (upper left), CFPM (lower left) and genipin solution (lower right) were tested against **(A)** *E.coli* and **(B)** *S.aureus*. **(C)** Diameter of inhibition zones.

TABLE 2 Quantification of organic acid in CFPM of HJ-S2.

Organic acid	Lactic acid	Acetic acid	Propionic acid	Butyric acid
Concentrations(mg/L)	26953.20	4830.54	181.89	86.27
RSD%	0.17%	0.16%	1.11%	4.14%

solutions ensure that the absorptive capacity of the hydrogel is fully utilized to maximize the absorption of exudates, secretions and other liquids that are not conducive to wound healing. Consequently, PM@CS hydrogel demonstrated unique advantages in specific medical scenarios.

Figure 4D shows the biodegradability of PM@CS hydrogel compared to Pure CS hydrogel. In the first 7 days, PM@CS hydrogel degraded slower than chitosan hydrogel in all kinds of solutions, illustrating that PM@CS hydrogel is more endurable against wound environment than Pure CS hydrogel. Enzyme degradation process was much faster. Both hydrogels were degraded completely with 7 days. While in DI water and SBF, there were part of the hydrogel remained nondegraded in day 7. PM@CS hydrogel in DI water remained undegraded in day 14, showing sustainable resistance to complete degradation. The results showed that after loading PMs of HJ-S2 into PM@CS hydrogel, the sustainability of the hydrogel in several different environment similar to human skin significantly increased. Therefore, when PM@CS hydrogel be applied to clinical

10.3389/fmats.2025.1573222

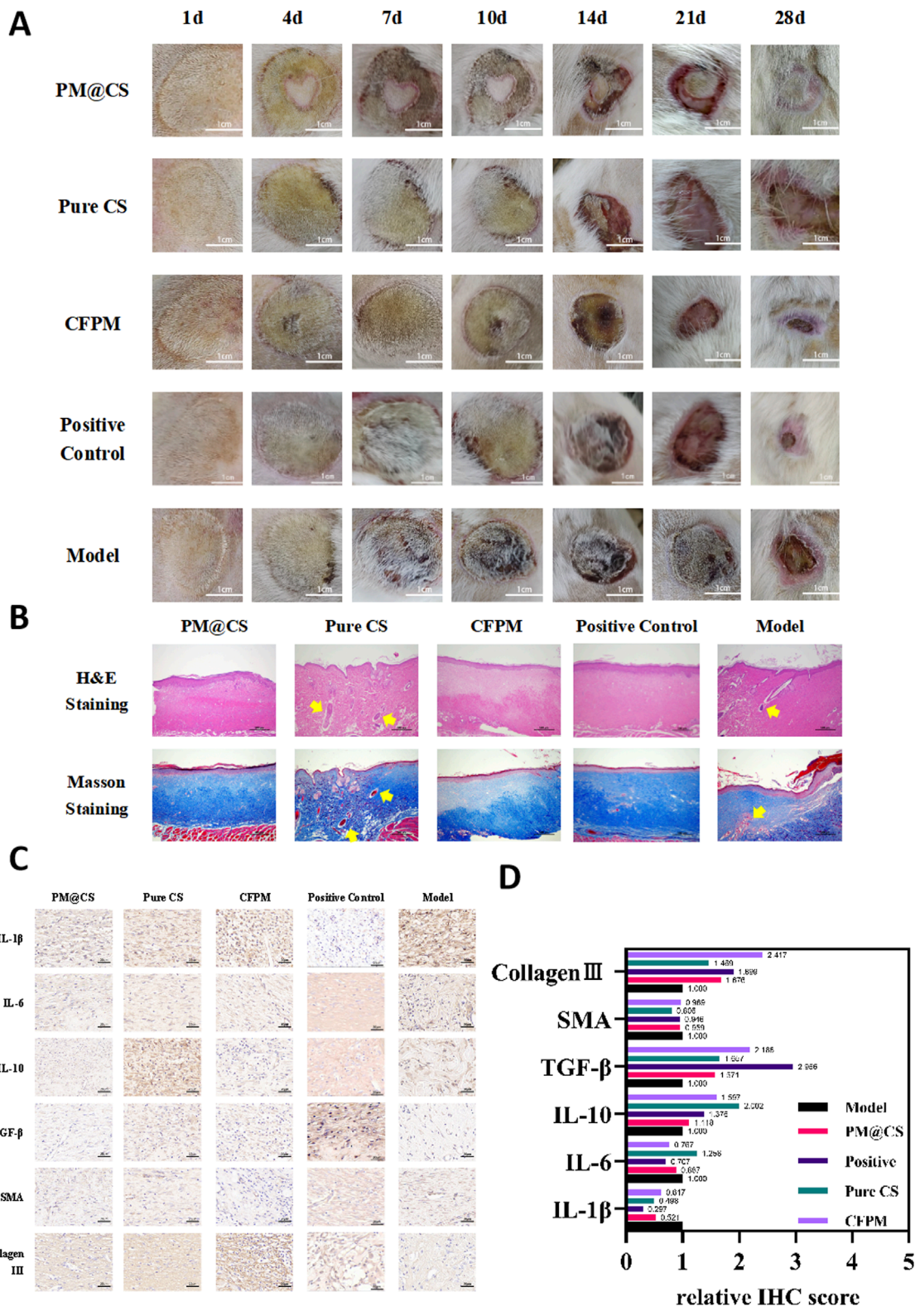

FIGURE 6
Effect of PM@CS hydrogel on burn wound healing. **(A)** Photographs of burn wound area after treatment. **(B)** H&E and Masson staining of skin tissues. **(C)** Immunohistochemical staining. **(D)** Relative score of IHC.

10.3389/fmats.2025.1573222

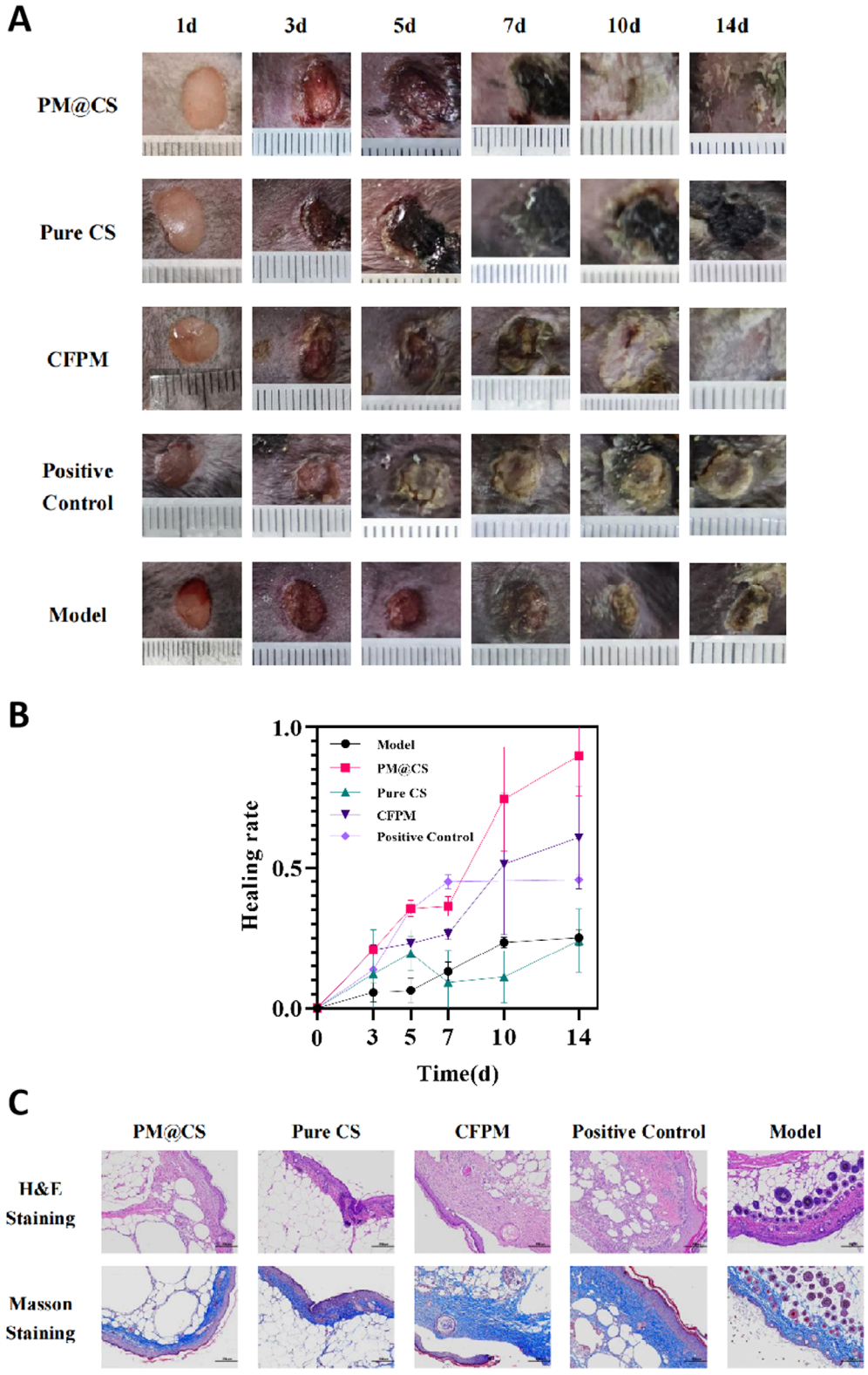

FIGURE 7
Effect of PM@CS hydrogel on diabetic wound healing. **(A)** wound healing process of each group. **(B)** Healing rate of the wounds within 14 days treatment. **(C)** Histology of the wounds treated by PM@CS, Pure CS, CFPM and Human EGF gel.

use in the future, it will preserve a longer effect on maintaining a benificial environment for wound healing.

Combined with the above water content, swelling performance and rheological performance test results, due to the presence of PMs of HJ-S2, the PM@CS hydrogel has better stability than Pure CS hydrogel in terms of slower uptake and release of external liquids as well as its own degradation, and it can ensure its own stabilized structure under the deformation of external forces. PMs of HJ-S2 may enhance the internal structure of chitosan hydrogel by participating in crosslinking reactions and form more crosslinked structures. CS molecules possess an abundance of positively charged amino groups ($-NH_2$), whereas PMs typically contain negatively charged groups (e.g., -COOH). These two components form ionic bonds via electrostatic interactions, thereby enhancing the crosslinking density of the hydrogel network (Obradović et al., 2015). Simultaneously, the hydroxyl (-OH) and amino groups of CS can establish hydrogen bonds with polar groups (e.g., -OH, -COOH) present in PMs, further stabilizing the three-dimensional network structure of the hydrogel. Furthermore, the organic acids (e.g., lactic acid) generated through probiotic fermentation decrease the local pH, thereby facilitating the protonation of chitosan ($-NH_3^+$) and enhancing its ionic cross-linking with anionic polymers. Simultaneously, the acidic environment may trigger hydrophobic interactions between chitosan molecules, further stabilizing the structure (Huang et al., 2023). Last but not least, biomacromolecules, including polysaccharides and proteins present in fermentation products, can form interpenetrating networks (IPN) with chitosan. This interaction enhances the structural integrity of hydrogels via physical entanglement or chemical coupling (Yucel Falco et al., 2017). In future study, we will focused on the detailed mechanisms of how PMs of HJ-S2 improves the stability of hydrogel.

3.2 Antimicrobial properties of PM@CS hydrogels and CFPM, and the organic acid compound characterization

The antibacterial ability of PM@CS hydrogel was tested by measuring the diameter of inhibition zone against *E.coli* and *S.aureus.* The result showed that the bacteria colonies were significantly reduced when contacting PM@CS hydrogel and CFPM of HJ-S2, indicating that PM@CS hydrogel and CFPM strongly inhibited the growth of *E.coli* and *S.aureus.* Pure CS hydrogel and genipin solution showed almost no inhibition against pathogen bacteria. Figures 5A,B shows the inhibition zones of each group. The diameter of inhibition zone was measured (Figure 5C). The efficacious antibacterial effect may be attributed to the secretion of organic acids or peptides in the metabolic process.

To further investigate the latent factors contributing to the inhibition of pathogenic bacteria, the quantification of four organic acids in the cell-free probiotic metabolites (CFPM) is presented in Table 2 and Supplementary Figure S1. The results are reported as concentrations along with the relevant standard deviation (RSD). Notably, there was significant production of acetic acid and lactic acid, whereas the production of propionic acid and butyric acid was relatively limited. The antibacterial mechanism of lactic acid and short-chain fatty acids is under ongoing research. According to existing research reports, lactic acid and short-chain fatty acids primarily exert their antibacterial effects by disrupting the structural integrity of bacterial cells (Ye et al., 2025). At the same time, some short-chain fatty acids are reported to have the ability to enter bacterial cells through free diffusion, reducing intracellular pH and inhibiting the metabolism of some macromolecules, and thus affect the growth and reproduction of bacteria (Akhtar et al., 2022; Cheung Lam et al., 2016; Hays et al., 2024). The high content of lactic acid and short-chain fatty acids in CFPM of HJ-S2 may contribute to its effective antibacterial activity against *E. coli* and *S. aureus* by destructing bacterial cell membrane and immodulating bacterial intracellular pH. In future studies, we intend to further investigate and isolate the bioactive bacteriostatic substances present in CFPM of HJ-S2 and elucidate their mechanisms of action.

3.3 Promotion of wound healing efficacy of hydrogels

The burn wounds of rats were photoed at 1, 4, 7, 10, 14, 21 and 28 days post-wounding to evaluate the recovery rate (Figure 6A). The PM@CS hydrogel-treated group showed better wound closure than other groups, while positive control group showed the same healing effects. Under the cooperative effect of CFPM of HJ-S2 and chitosan, the wound recovered rapidly. The CFPM-treated group showed better wound closure than control group, while Pure CS hydrogel-treated group experienced even worse wound closure than control group. Due to its acidity, Pure CS hydrogel demonstrated a destructive effect on wounded area, which delayed the wound healing process.

Tissue sections taken were going under H&E staining and Masson staining to examine the cellular response within the tissue of wound area (Figure 6B). The PM@CS hydrogel group and the CFPM group, as well as positive control group, demonstrated effective tissue regeneration, with well-organized cells and optimal densification. The collagen fibers were abundant and neatly arranged. In contrast, the chitosan hydrogel group exhibited tissue cells and collagen fibers that were loosely organized and disorganized, with internal cavities and visible inflammatory cells (which the ticks point to in Figure 6B). This resulted in a less favorable recovery compared to the control group. In the model group, the cells were loosely arranged, and a small number of inflammatory cells could still be observed. Immunohistochemical staining was employed to assess the expression of cytokines and proteins associated with inflammation and tissue regeneration (Figure 6C). ,Relative IHC scores were utilized to quantify the expression levels (Figure 6D). Following the application of PM@CS hydrogel and CFPM, the expression levels of pro-inflammatory factors IL-1β and IL-6 were found to be decreased, while the expression level of the anti-inflammatory factor IL-10 was increased. This suggests that the inflammatory response of the wound was reduced. The expression levels of epidermal growth factor, TGF-β, and collagen III all demonstrated an increase, indicating that the wound exhibited a notable recovery following the administration of the hydrogel, which represented a significant improvement in comparison to the control group.

When viewed in conjunction with the wound healing images and tissue staining outcomes, it is evident that the PM@CS hydrogel

and CFPM facilitated the wound healing process in rats with third-degree burn wounds.In the burn model, PM@CS hydrogel does not exhibit a significant advantage compared to CFPM. The slow release of active ingredients in PM@CS hydrogels may be attributed to their densely cross-linked networks or diffusion resistance (Zhao et al., 2023b). In future studies, we will concentrate on investigating the slow-release characteristics of hydrogels, enhancing the release rate of their components, and optimizing the hydrogel's performance for burn wound healing applications.

As for diabetic wound healing, the wounds of the mice displayed discrepant healing progress (Figure 7A). While in the inflammatory stage, the early stage of the whole wound healing process (day 3), the PM@CS group, CFPM group and positive control group observed different level of reduced inflammation response. Scabs were observed in all groups at day 5. While the wounds of all other groups were recovered steadily, Pure CS group showed poor recovery rate and even suffered ulcerating in day 7. Almost complete wound healing was observed in PM@CS-treated group and CFPM-treated group, while in model group, the scabs did not come off yet, signifying that the CFPM of HJ-S2 and PM@CS hydrogel played an important role in accelerating diabetic wound healing process. The wound healing rate over 14 days after wounded was shown in Figure 7B. PM@CS-treated group showed the best healing rate (89.95%), followed by CFPM-treated group (60.83%). After 14 days administration, positive control group (45.71%) also recovered better than model group (25.13%). Pure CS hydrogel-treated group showed the slowest healing rate (24.14%), even worse than model group. Considering the destructive effect of Pure CS hydrogel on burn wounds and the slow healing process on diabetic wounds, it was discovered that Pure CS hydrogel was harmful to wound environment, thus lead to delayed wound healing. Although it has been reported that acetic acid (used to dissolve chitosan in Pure CS hydrogel) possess antibacterial and antifungal ability (Elhage et al., 2021). When exceeding certain concentration, resulting in extremely low pH, acetic acid in Pure CS hydrogel turns out to be a hindrance to wound healing.

Tissue staining images of the diabetic wounds were shown in Figure 7C. The mice in the PM@CS hydrogel- and CFPM-treated group exhibited superior skin tissue regeneration at the wound site, with more compactly arranged fibrous tissues and a reduced presence of inflammatory cells. The positive control group also demonstrated enhanced skin tissue repair following the administration of Human EGF gel. However, the mice in the Pure CS group displayed inadequate tissue regeneration with loosely arranged fibers. The result showed that PM@CS hydrogel and CFPM also played an effective role in the recovery of skin wounds in diabetic mice.

4 Conclusion

In conclusion, our team has successfully created a chitosan-based hydrogel capable of incorporating cell-free probiotic metabolites CFPM from marine-derived probiotics *L. plantarum* HJ-S2, thereby establishing a platform for the delivery of substances conducive to wound healing. The synthesis of the PM@CS hydrogel does not necessitate the use of any toxic chemical agents, and the production process is both straightforward and environmentally benign. Thermalgravimetric and rheological assessments indicate that the PM@CS hydrogel is adaptable in its formulation while maintaining a stable structural integrity across diverse environmental conditions. The PM@CS hydrogel exhibits a superior antibacterial efficacy against *E.coli* and *S.aureus*. The inhibitory properties against pathogens may be attributed to the main organic acid compound such as lactic acid and acetic acid in the cell-free metabolites (CFPM) of HJ-S2, as other researchers have reported the similar findings (Mani-López et al., 2022; Feng et al., 2022).

Compared to Pure CS hydrogel, PM@CS hydrogel has been demonstrated to be more efficacious in the healing of burn wounds, with minimal adverse effects on the wound area. Application of the PM@CS hydrogel to the wound site has been observed to mitigate the inflammatory response, with a notable enhancement in the rate of recovery and tissue regeneration. The same trend has also been observed in diabetic wound healing test. When contrasted with other chitosan-based hydrogels, the PM@CS hydrogel stands out due to its enrichment with metabolically active probiotic derivatives, providing a novel and potent therapeutic supplement for the management of burn wounds and the treatment of diabetic wounds.

Data availability statement

The original contributions presented in the study are included in the article/Supplementary Material, further inquiries can be directed to the corresponding author.

Ethics statement

The animal study was approved by the Institutional Committee on the Care and Use of Animals of the Third Institute of Oceanography, Ministry of Natural Resources. The study was conducted in accordance with the local legislation and institutional requirements.

Author contributions

YiL: Conceptualization, Data curation, Formal Analysis, Investigation, Methodology, Writing – original draft. XT: Conceptualization, Methodology, Supervision, Visualization, Writing – review and editing. YaL: Conceptualization, Data curation, Investigation, Methodology, Writing – original draft. XC: Conceptualization, Data curation, Writing – review and editing. LW: Conceptualization, Data curation, Writing – review and editing. YS: Visualization, Writing – review and editing. WH: Visualization, Writing – review and editing. JL: Visualization, Writing – review and editing. QH: Visualization, Writing – review and editing. PW: Funding acquisition, Project administration, Supervision, Validation, Writing – review and editing.

Funding

The author(s) declare that financial support was received for the research and/or publication of this article. This study was supported by the Youth Science and Technology Innovation Program of Xiamen Ocean and Fisheries Development Special Funds (grant number: 23YYZP010QCA18), Innovation Research and Development Special Funds of the Municipality-province-ministry Co-constructed (grant number: GJZX-HYSW-2024-09).

Conflict of interest

Authors WH and JL were employed by China Tobacco Fujian Industrial CO., LTD.

Author QH was employed by Fujian Huijing Biological Technology CO., LTD.

The remaining authors declare that the research was conducted in the absence of any commercial or financial relationships that could be construed as a potential conflict of interest.

Generative AI statement

The author(s) declare that no Generative AI was used in the creation of this manuscript.

Publisher's note

All claims expressed in this article are solely those of the authors and do not necessarily represent those of their affiliated organizations, or those of the publisher, the editors and the reviewers. Any product that may be evaluated in this article, or claim that may be made by its manufacturer, is not guaranteed or endorsed by the publisher.

Supplementary material

The Supplementary Material for this article can be found online at: https://www.frontiersin.org/articles/10.3389/fmats.2025.1573222/full#supplementary-material

References

Abazari, M., Ghaffari, A., Rashidzadeh, H., Badeleh, S. M., and Maleki, Y. (2022). A systematic review on classification, identification, and healing process of burn wound healing. *Int. J. Low. Extrem Wounds* 21, 18–30. doi:10.1177/1534734620924857

Akhtar, M., Naqvi, S. U., Liu, Q., Pan, H., Ma, Z., Kong, N., et al. (2022). Short chain fatty acids (SCFAs) are the potential immunomodulatory metabolites in controlling Staphylococcus aureus-mediated mastitis. *Nutrients* 14, 3687. doi:10.3390/nu14183687

AL-Saafin, B. A., AL-Bakri, A. G., Abdelrazig, S., and Dahabiyeh, L. A. (2023). Investigating the effect of the probiotic Lactobacillus plantarum and the prebiotic fructooligosaccharides on *Pseudomonas aeruginosa* metabolome, virulence factors and biofilm formation as potential *quorum* sensing inhibitors. *Microb. Pathog.* 177, 106057. doi:10.1016/j.micpath.2023.106057

Andrade Del Olmo, J., Perez-Alvarez, L., Saez-Martinez, V., Benito-Cid, S., Ruiz-Rubio, L., Perez-Gonzalez, R., et al. (2022). Wound healing and antibacterial chitosan-genipin hydrogels with controlled drug delivery for synergistic anti-inflammatory activity. *Int. J. Biol. Macromol.* 203, 679–694. doi:10.1016/j.ijbiomac.2022.01.193

Broussard, K. C., and Powers, J. G. (2013). Wound dressings: selecting the most appropriate type. *Am. J. Clin. Dermatol* 14, 449–459. doi:10.1007/s40257-013-0046-4

Cheung Lam, A. H., Sandoval, N., Wadhwa, R., Gilkes, J., Do, T. Q., Ernst, W., et al. (2016). Assessment of free fatty acids and cholesteryl esters delivered in liposomes as novel class of antibiotic. *BMC Res. Notes* 9, 337. doi:10.1186/s13104-016-2138-8

Church, D., Elsayed, S., Reid, O., Winston, B., and Lindsay, R. (2006). Burn wound infections. *Clin. Microbiol. Rev.* 19, 403–434. doi:10.1128/cmr.19.2.403-434.2006

Chu, W., Wang, P., Ma, Z., Peng, L., Guo, C., Fu, Y., et al. (2023). Lupeol-loaded chitosan-Ag(+) nanoparticle/sericin hydrogel accelerates wound healing and effectively inhibits bacterial infection. *Int. J. Biol. Macromol.* 243, 125310. doi:10.1016/j.ijbiomac.2023.125310

D'Abbondanza, J. A., and Shahrokhi, S. (2021). Burn infection and burn sepsis. *Surg. Infect. (Larchmt)* 22, 58–64. doi:10.1089/sur.2020.102

Elhage, K. G., St. Claire, K., and Daveluy, S. (2021). Acetic acid and the skin: a review of vinegar in dermatology. *Int. J. Dermatology* 61, 804–811. doi:10.1111/ijd.15804

Evers, L. H., Bhavsar, D., and Mailander, P. (2010). The biology of burn injury. *Exp. Dermatol* 19, 777–783. doi:10.1111/j.1600-0625.2010.01105.x

Eze, O. C., Berebon, D. P., Emencheta, S. C., Evurani, S. A., Okorie, C. N., BalcãO, V. M., et al. (2023). Therapeutic potential of marine probiotics: a survey on the anticancer and antibacterial effects of pseudoalteromonas spp. *Pharm. (Basel)* 16, 1091. doi:10.3390/ph16081091

Feng, L., Xu, M., Zeng, W., Zhang, X., Wang, S., Yao, Z., et al. (2022). Evaluation of the antibacterial, antibiofilm, and anti-virulence effects of acetic acid and the related mechanisms on colistin-resistant *Pseudomonas aeruginosa*. *BMC Microbiol.* 22, 306. doi:10.1186/s12866-022-02716-6

Forbes, J. M., and Cooper, M. E. (2013). Mechanisms of diabetic complications. *Physiol. Rev.* 93, 137–188. doi:10.1152/physrev.00045.2011

Gong, Y., Wang, P., Cao, R., Wu, J., Ji, H., Wang, M., et al. (2023). Exudate absorbing and antimicrobial hydrogel integrated with multifunctional curcumin-loaded magnesium polyphenol network for facilitating burn wound healing. *ACS Nano* 17, 22355–22370. doi:10.1021/acsnano.3c04556

Grip, J., Steene, E., Engstad, R. E., Hart, J., Bell, A., SkjæVELAND, I., et al. (2021). Development of a novel beta-glucan supplemented hydrogel spray formulation and wound healing efficacy in a db/db diabetic mouse model. *Eur. J. Pharm. Biopharm.* 169, 280–291. doi:10.1016/j.ejpb.2021.10.013

Hays, K. E., Pfaffinger, J. M., and Ryznar, R. (2024). The interplay between gut microbiota, short-chain fatty acids, and implications for host health and disease. *Gut Microbes* 16, 2393270. doi:10.1080/19490976.2024.2393270

Heimbuck, A. M., Priddy-Arrington, T. R., Padgett, M. L., Llamas, C. B., Barnett, H. H., Bunnell, B. A., et al. (2019). Development of responsive chitosan-genipin hydrogels for the treatment of wounds. *ACS Appl. Bio Mater* 2, 2879–2888. doi:10.1021/acsabm.9b00266

Huang, Y., Zhang, L., Hu, J., and Liu, H. (2023). Improved loading capacity and viability of probiotics encapsulated in alginate hydrogel beads by *in situ* cultivation method. *Foods* 12, 2256. doi:10.3390/foods12112256

Kamolz, L.-P., and Hecker, A. (2023). Molecular mechanisms related to burns, burn wound healing and scarring. *Int. J. Mol. Sci.* 24, 8785. doi:10.3390/ijms24108785

Khayrova, A., Lopatin, S., and Varlamov, V. (2021). Obtaining chitin, chitosan and their melanin complexes from insects. *Int. J. Biol. Macromol.* 167, 1319–1328. doi:10.1016/j.ijbiomac.2020.11.086

Kim, S. K., Bhatnagar, I., and Kang, K. H. (2012). Development of marine probiotics: prospects and approach. *Adv. Food Nutr. Res.* 65, 353–362. doi:10.1016/B978-0-12-416003-3.00023-8

Kuhn, T., Aljohmani, A., Frank, N., Zielke, L., Mehanny, M., Laschke, M. W., et al. (2024). A cell-free, biomimetic hydrogel based on probiotic membrane vesicles ameliorates wound healing. *Journal of controlled release: official journal of the Controlled Release Society* 365, 969–980. doi:10.1016/j.jconrel.2023.12.011

Liang, Y., He, J., and Guo, B. (2021). Functional hydrogels as wound dressing to enhance wound healing. *ACS Nano* 15, 12687–12722. doi:10.1021/acsnano.1c04206

Li, H., Jia, M., Qi, Q., and Wang, Q. (2023). Engineered probiotic Lactobacillus plantarum WCSF I for monitoring and treatment of *Staphylococcus aureus* infection. *Microbiol. Spectr.* 11, e0182923. doi:10.1128/spectrum.01829-23

Liu, L., Wang, H., Chen, X., Zhang, Y., Zhang, H., and Xie, P. (2023). Gut microbiota and its metabolites in depression: from pathogenesis to treatment. *EBioMedicine* 90, 104527. doi:10.1016/j.ebiom.2023.104527

Li, Z., Qian, C., Zheng, X., Qi, X., Bi, J., Wang, H., et al. (2024). Collagen/chitosan/genipin hydrogel loaded with phycocyanin nanoparticles and ND-336 for diabetic wound healing. *Int. J. Biol. Macromol.* 266, 131220. doi:10.1016/j.ijbiomac.2024.131220

Mani-LóPEZ, E., Arrioja-BretóN, D., and LóPEZ-Malo, A. (2022). The impacts of antimicrobial and antifungal activity of cell-free supernatants from lactic acid bacteria *in vitro* and foods. *Compr. Rev. Food Sci. Food Saf.* 21, 604–641. doi:10.1111/1541-4337.12872

Marco, M. L., Heeney, D., Binda, S., Cifelli, C. J., Cotter, P. D., Foligné, B., et al. (2017). Health benefits of fermented foods: microbiota and beyond. *Curr. Opin. Biotechnol.* 44, 94–102. doi:10.1016/j.copbio.2016.11.010

Markiewicz-Gospodarek, A., Kozioł, M., Tobiasz, M., Baj, J., Radzikowska-BüCHNER, E., and Przekora, A. (2022). Burn wound healing: clinical complications, medical care, treatment, and dressing types: the current state of knowledge for clinical practice. *Int. J. Environ. Res. Public Health* 19, 1338. doi:10.3390/ijerph19031338

Mei, L., Zhang, D., Shao, H., Hao, Y., Zhang, T., Zheng, W., et al. (2022). Injectable and self-healing probiotics-loaded hydrogel for promoting superbacteria-infected wound healing. *ACS applied materials & interfaces* 14 18, 20538–20550. doi:10.1021/acsami.1c23713

Mekky, A. F., Hassanein, W. A., Reda, F. M., and Elsayed, H. M. (2022). Anti-biofilm potential of Lactobacillus plantarum Y3 culture and its cell-free supernatant against multidrug-resistant uropathogen *Escherichia coli* U12. *Saudi J. Biol. Sci.* 29, 2989–2997. doi:10.1016/j.sjbs.2022.01.014

Ming, Z., Han, L., Bao, M., Zhu, H., Qiang, S., Xue, S., et al. (2021). Living bacterial hydrogels for accelerated infected wound healing. *Advanced science (Weinheim, Baden-Wurttemberg, Germany)* 8 (24), e2102545. doi:10.1002/advs.202102545

Obradović, N. S., Krunić, T. Ž., Trifković, K. T., Bulatović, M. L., Rakin, M. P., Rakin, M. B., et al. (2015). Influence of chitosan coating on mechanical stability of biopolymer carriers with probiotic starter culture in fermented whey beverages. *Int. J. Polym. Sci.* 2015, 1–8. doi:10.1155/2015/732858

Oryan, A., Alemzadeh, E., Mohammadi, A. A., and Moshiri, A. (2019). Healing potential of injectable Aloe vera hydrogel loaded by adipose-derived stem cell in skin tissue-engineering in a rat burn wound model. *Cell Tissue Res.* 377, 215–227. doi:10.1007/s00441-019-03015-9

Ozhathil, D. K., Tay, M. W., Wolf, S. E., and Branski, L. K. (2021). A narrative review of the history of skin grafting in burn care. *Med. Kaunas.* 57, 380. doi:10.3390/medicina57040380

Patel, B. K., Patel, K. H., Huang, R. Y., Lee, C. N., and Moochhala, S. M. (2022). The gut-skin microbiota Axis and its role in diabetic wound healing—a review based on current literature. *Int. J. Mol. Sci.* 23, 2375. doi:10.3390/ijms23042375

Peers, S., Alcouffe, P., Montembault, A., and LadavièRE, C. (2020). Embedment of liposomes into chitosan physical hydrogel for the delayed release of antibiotics or anaesthetics, and its first ESEM characterization. *Carbohydr. Polym.* 229, 115532. doi:10.1016/j.carbpol.2019.115532

Peixoto, R. S., Sweet, M., Villela, H. D. M., Cardoso, P., Thomas, T., Voolstra, C. R., et al. (2021). Coral probiotics: premise, promise, prospects. *Annu. Rev. Anim. Biosci.* 9, 265–288. doi:10.1146/annurev-animal-090120-115444

Priddy-Arrington, T. R., Edwards, R. E., Colley, C. E., Nguyen, M. M., Hamilton-Adaire, T., and Caldorera-Moore, M. E. (2023). Characterization and optimization of injectable *in situ* crosslinked chitosan-genipin hydrogels. *Macromol. Biosci.* 23, e2200505. doi:10.1002/mabi.202200505

Rao, W., Wu, J., Fang, Z., Chen, Z., Wu, J., and Fang, X. (2024). Antibacterial mechanism of metabolites of Lactobacillus plantarum against Pseudomonas lundensis and their application in dry-aged beef preservation. *Food Chem.* 460, 140463. doi:10.1016/j.foodchem.2024.140463

Rowan, M. P., Cancio, L. C., Elster, E. A., Burmeister, D. M., Rose, L. F., Natesan, S., et al. (2015). Burn wound healing and treatment: review and advancements. *Crit. Care* 19, 243. doi:10.1186/s13054-015-0961-2

Uberoi, A., Mccready-Vangi, A., and Grice, E. A. (2024). The wound microbiota: microbial mechanisms of impaired wound healing and infection. *Nat. Rev. Microbiol.* 22, 507–521. doi:10.1038/s41579-024-01035-z

Varghese, F., Bukhari, A. B., Malhotra, R., and DE, A. (2014). IHC Profiler: an open source plugin for the quantitative evaluation and automated scoring of immunohistochemistry images of human tissue samples. *PLoS One* 9, e96801. doi:10.1371/journal.pone.0096801

Wang, Y., Beekman, J., Hew, J., Jackson, S., Issler-Fisher, A. C., Parungao, R., et al. (2018). Burn injury: challenges and advances in burn wound healing, infection, pain and scarring. *Adv. Drug Deliv. Rev.* 123, 3–17. doi:10.1016/j.addr.2017.09.018

Wan, J., Wu, P., Huang, J., Huang, S., Huang, Q., and Tang, X. (2023). Characterization and evaluation of the cholesterol-lowering ability of Lactiplantibacillus plantarum HJ-S2 isolated from the intestine of Mesoplodon densirostris. *World J. Microbiol. Biotechnol.* 39, 199. doi:10.1007/s11274-023-03637-w

WieëRS, G., Belkhir, L., Enaud, R., Leclercq, S., Philippart DE Foy, J. M., Dequenne, I., et al. (2019). How probiotics affect the microbiota. *Front. Cell Infect. Microbiol.* 9, 454. doi:10.3389/fcimb.2019.00454

Womersley, F., Hancock, J., Perry, C. T., and Rowat, D. (2021). Wound-healing capabilities of whale sharks (Rhincodon typus) and implications for conservation management. *Conserv. Physiol.* 9, coaa120. doi:10.1093/conphys/coaa120

Ye, D., Ren, J., Zhang, Y., Wang, X., Guo, J., Li, B., et al. (2025). Lactic acid/tartaric acid-maltitol antibacterial activity against spoilage bacteria and prevention of yellowing and wilting in spinach and oilseed rape. *Food Chem.* 471, 142557. doi:10.1016/j.foodchem.2024.142557

Younes, I., and Rinaudo, M. (2015). Chitin and chitosan preparation from marine sources. Structure, properties and applications. *Mar. Drugs* 13, 1133–1174. doi:10.3390/md13031133

Yucel Falco, C., Falkman, P., Risbo, J., CáRDENAS, M., and Medronho, B. (2017). Chitosan-dextran sulfate hydrogels as a potential carrier for probiotics. *Carbohydr. Polym.* 172, 175–183. doi:10.1016/j.carbpol.2017.04.047

Zhao, C., Yang, Q., Tang, R., Li, W., Wang, J., Yang, F., et al. (2023a). DNA methyltransferase 1 deficiency improves macrophage motility and wound healing by ameliorating cholesterol accumulation. *NPJ Regen. Med.* 8, 29. doi:10.1038/s41536-023-00306-2

Zhao, J., Qiu, P., Wang, Y., Wang, Y., Zhou, J., Zhang, B., et al. (2023b). Chitosan-based hydrogel wound dressing: from mechanism to applications, a review. *Int. J. Biol. Macromol.* 244, 125250. doi:10.1016/j.ijbiomac.2023.125250